Space-time domain decomposition methods and a posteriori error estimates for the heat equation

Sarah Ali Hassan, Caroline Japhet, Michel Kern, Martin Vohralík

▶ **To cite this version:**

Sarah Ali Hassan, Caroline Japhet, Michel Kern, Martin Vohralík. Space-time domain decomposition methods and a posteriori error estimates for the heat equation. EDP-NORMANDIE 2017 - VIe Colloque Edp-normandie, Oct 2017, Caen, France. pp.1-18. hal-01702428

HAL Id: hal-01702428
https://inria.hal.science/hal-01702428

Submitted on 6 Feb 2018

HAL is a multi-disciplinary open access archive for the deposit and dissemination of scientific research documents, whether they are published or not. The documents may come from teaching and research institutions in France or abroad, or from public or private research centers.

L'archive ouverte pluridisciplinaire **HAL**, est destinée au dépôt et à la diffusion de documents scientifiques de niveau recherche, publiés ou non, émanant des établissements d'enseignement et de recherche français ou étrangers, des laboratoires publics ou privés.

Space-time domain decomposition methods and a posteriori error estimates for the heat equation*

Sarah Ali Hassan†, Caroline Japhet‡, Michel Kern†, Martin Vohralík†

Abstract

This paper develops a posteriori estimates for global-in-time, nonoverlapping domain decomposition (DD) methods for heterogeneous diffusion problems. The method uses optimized Schwarz waveform relaxation (OSWR) with Robin transmission conditions on the space-time interface between subdomains, and a lowest-order Raviart–Thomas–Nédélec discretization in the subdomains. Our estimates yield a guaranteed and fully computable upper bound on the error measured in the space-time energy norm of [19, 20], at each iteration of the space-time DD algorithm, where the spatial discretization, the time discretization, and the domain decomposition error components are estimated separately. Thus, an adaptive space-time DD algorithm is proposed, wherein the iterations are stopped when the domain decomposition error does not affect significantly the global error, allowing important savings in terms of the number of domain decomposition iterations while guaranteeing a user-given precision. Numerical results for a two-dimensional heat equation are presented to illustrate the efficiency of our a posteriori estimates and the performance of the adaptive stopping criteria for the space-time DD algorithm.

Key words: Heterogeneous diffusion, mixed finite element method, space-time domain decomposition, discontinuous Galerkin in time, optimized Robin transmission conditions, a posteriori error estimate, stopping criteria

1 Introduction

Let $\Omega \subset \mathbb{R}^d$, $d = 2, 3$, be a polygonal (polyhedral if $d = 3$) domain (open, bounded and connected set) with Lipschitz-continuous boundary $\partial\Omega$ decomposed into two connected sets Γ^{D} and Γ^{N} with Γ^{D} of nonzero $(d-1)$-dimensional measure.

We consider space-time domain decomposition strategies for solving the following diffusion problem with final time $T > 0$: find the potential p and the flux $\mathbf{u}$ such that:

$$\mathbf{u} = -\nabla p \quad \text{in} \quad \Omega \times (0,T), \tag{1.1a}$$

$$\frac{\partial p}{\partial t} + \nabla\cdot\mathbf{u} = f \quad \text{in} \quad \Omega \times (0,T), \tag{1.1b}$$

$$p = g_{\mathrm{D}} \quad \text{on} \quad \Gamma^{\mathrm{D}} \times (0,T), \tag{1.1c}$$

$$-\mathbf{u}\cdot\mathbf{n} = g_{\mathrm{N}} \quad \text{on} \quad \Gamma^{\mathrm{N}} \times (0,T), \tag{1.1d}$$

$$p(\cdot,0) = p_0 \quad \text{in} \quad \Omega, \tag{1.1e}$$

where $g_{\mathrm{D}} \in H^{\frac{1}{2}}(\Gamma^{\mathrm{D}} \times (0,T)) \cap C^0(\overline{\Gamma}^{\mathrm{D}} \times (0,T))$, $g_{\mathrm{N}} \in L^2(\Gamma^{\mathrm{N}} \times (0,T))$, and where $f \in L^2(\Omega \times (0,T))$, and $p_0 \in H^1(\Omega)$ with $p_0|_{\Gamma^{\mathrm{D}}} = g_{\mathrm{D}}(\cdot,0)|_{\Gamma^{\mathrm{D}}}$. Here $\mathbf{n}$ is the outward unit normal vector to $\partial\Omega$.

*This work was supported by ANDRA, the French agency for nuclear waste management, and by the ANR project DEDALES under grant ANR-14-CE23-0005. It has also received funding from the European Research Council (ERC) under the European Union's Horizon 2020 research and innovation program (grant agreement No 647134 GATIPOR).

†Inria Paris, 2 rue Simone Iff, 75589 Paris, France & Université Paris-Est, CERMICS (ENPC), 77455 Marne-la-Vallée 2, France sarah.ali-hassan@inria.fr,michel.kern@inria.fr,martin.vohralik@inria.fr.

‡Université Paris 13, Sorbonne Paris Cité, LAGA, CNRS (UMR 7539), 93430, Villetaneuse, France japhet@math.univ-paris13.fr.

In this article we are concerned with global-in-time optimized Schwarz method which uses optimized Schwarz waveform relaxation (OSWR) introduced in [26, 37]. The OSWR algorithm is an iterative method that computes in the subdomains over the whole time interval, exchanging space-time boundary data through more general (Robin or Ventcell) transmission operators in which coefficients can be optimized to improve convergence rates [31, 37, 10, 11]. This method allows to different time discretizations in subdomains, and needs a very small number of iterations to converge, see [25, 27] and the references therein, and [28, 29, 30] in the context of mixed finite elements. The OSWR algorithm can actually be reformulated as a block-Jacobi method applied to a space-time interface problem, see [17] and the references therein, see also [28, 3, 4], and on can replace the block-Jacobi algorithm by other by various iterative methods, such as Krylov-type methods like GMRES.

The present paper intends to give a posteriori estimates with a guaranteed and fully computable upper bound on the error at each iteration of the space-time DD algorithm. In the context of algebraic iterative solvers, several methods with residual-based estimates have been proposed, see [9, 6, 7], and [39, 38, 43] for goal-oriented a posteriori error estimates. Then, in [21], a general framework for any numerical method and algebraic solver has been introduced, following [32]. Extensions of this framework to coupled unsteady nonlinear and degenerate problems are given in [12, 15], and to parabolic problems in [20, 19]. It uses H^1-conforming reconstruction of the potential, continuous and piecewise affine in time, and an equilibrated $H(div)$-conforming reconstruction of the flux, piecewise constant in time. A guaranteed and fully computable upper bound on the error measured in the energy norm augmented by a dual norm of the time derivative is derived (see [47, 20]), without unknown constants. In [20, 19] an equivalent norm is used, leading to local space-time efficiency.

In the context of non-overlapping domain decomposition algorithms, a posteriori error estimates for FETI [23] or BDD [36, 13] methods, have been proposed in [44, 45]. It is based on $H^1(\Omega)$-conforming potential and $\mathbf{H}(\mathrm{div},\Omega)$-conforming flux reconstructions, following [41, 34, 42, 22], that can be obtained when subdomain problems involve both Dirichlet and Neumann interface conditions on each domain decomposition (DD) iteration, as this is the case for FETI or BDD. For domain decomposition methods with Robin or Ventcell interface conditions, and where neither the conformity of the flux nor that of the potential is preserved (as long as the convergence is not reached), new a posteriori error estimates and stopping criteria has been introduced in [3, 1].

The purpose of this paper is to extend the techniques of [3] to the OSWR method for solving the heat equation. We give a general a posteriori error estimate with fully computable upper bound, distinguishing the spatial discretization, the temporal discretization, and the domain decomposition error components. This new adaptive space-time domain decomposition algorithm uses two H^1-conforming potential reconstructions (one globally on Ω, and one on each subdomain Ω_i), and an $\mathbf{H}(\mathrm{div},\Omega)$-conforming flux reconstruction. Details of the proof and of the potential and flux reconstructions are given in [4]. In the present contribution, we give numerical experiments for the heat equation to validate our adaptive method: we consider a test case where the exact solution is known and show the actual and estimated errors against the number of OSWR iterations and the corresponding effectivity indices. As mentioned above, the OSWR algorithm can be reformulated as a block-Jacobi method applied to a space-time interface problem, and one can replace block-Jacobi by GMRES. We give a comparison between the adaptive block-Jacobi (OSWR) algorithm and the adaptive GMRES algorithm. In the companion paper [4], our general a posteriori error estimate is extended to a diffusion problem with heterogeneous diffusion tensor and to a domain decomposition with different time grids, so as to adapt to different time scales in the subdomains; numerical results are shown in [4] for a two-dimensional problem with strong heterogeneities (where the exact solution is not known) and with local time stepping.

More precisely, this new adaptive space-time domain decomposition algorithm uses mixed finite elements (leading to mass conservation and flux continuity), and extends the a posteriori estimates of [33, 48, 2, 49, 40, 20, 19, 3]. It uses two H^1-conforming potential reconstructions, one is global over Ω and relies on the adjustement of the averaging operator $\mathcal{I}_{\mathrm{av}}$ for parabolic problems following [20], and the other introduces weights on the interfaces following [3] to separate the space-time DD and the discretization components. The method also uses a flux reconstruction that is globally $\mathbf{H}(\mathrm{div},\Omega)$-conforming, locally conservative in each mesh element, and piecewise constant in time. It relies on solving a simple coarse balancing problem, and then solving local Neumann problems in bands around the interfaces in each subdomain, following [3].

The remainder of this paper is organized as follows: in the next section we introduce some useful notation.

We present in Section 3 the multi-domain formulation using the OSWR algorithm, in the continuous case and in the fully discrete case using the mixed finite element method in space and the discontinuous Galerkin method of order zero in time. In Section 4, we derive a fully computable upper bound for the error between the exact and the approximate numerical solution on a given DD iteration, in the energy norm. In Section 5, results of 2D numerical experiments showing tight overall error control and important reduction of the number of space-time DD iterations are discussed.

2 Preliminaries

In this part we give the partition of the domain Ω as well as some function spaces following the notations introduced in [3, 4].

2.1 Partitions of the domain Ω

We suppose that the domain Ω is decomposed into $\mathcal{N}$ non-overlapping polygonal subdomains Ω_i, $i \in [\![1, \mathcal{N}]\!]$, such that $\overline{\Omega} = \bigcup_{i=1}^{\mathcal{N}} \overline{\Omega}_i$. For all $i \in [\![1, \mathcal{N}]\!]$, let $\Gamma_i^{\mathrm{N}} := \Gamma^{\mathrm{N}} \cap \partial\Omega_i$, $\Gamma_i^{\mathrm{D}} := \Gamma^{\mathrm{D}} \cap \partial\Omega_i$, and $\mathbf{n}_i$ be the unit outward-pointing normal of $\partial\Omega_i$. Let B^i be the set of neighbors of the subdomain Ω_i that share at least one edge if $d = 2$ with Ω_i (face if $d = 3$) and let $|B^i|$ be the cardinality of this set. Using this notation, we introduce the interface $\Gamma_{i,j} := \partial\Omega_i \cap \partial\Omega_j$, $j \in B^i$, between two adjacent subdomains Ω_i and Ω_j. Consequently, $\partial\Omega_i = \Gamma_i^{\mathrm{N}} \cup \Gamma_i^{\mathrm{D}} \cup \Gamma_i$ with $\Gamma_i := \bigcup_{j \in B^i} \Gamma_{i,j}$. We define $\Gamma := \bigcup_{i \in [\![1,\mathcal{N}]\!]} \Gamma_i$.

We then define $\mathcal{T}_h := \bigcup_{i=1}^{\mathcal{N}} \mathcal{T}_{h,i}$, where $\mathcal{T}_{h,i}$ is a regular triangulation of the subdomain Ω_i, such that $\overline{\Omega}_i = \bigcup_{K \in \mathcal{T}_{h,i}} K$, where $|\mathcal{T}_{h,i}|$ is the number of triangles (tetrahedra if d=3) in the i-th subdomain. We suppose that $\mathcal{T}_{h,i}$ is a conforming mesh, i.e., such that if K, $K' \in \mathcal{T}_{h,i}$, $K \neq K'$, then $K \cap K'$ is either an empty set or a common vertex or edge or face. For simplicity, we assume that $\mathcal{T}_h$ is conforming, although this assumption could be easily avoided by introducing the concept of a simplicial submesh (see e.g. [40, 18] and the references therein). We denote the set of all edges (faces if $d = 3$) of $\mathcal{T}_{h,i}$ by $\mathcal{E}_{h,i}$, and the set of all edges (faces) of $K \in \mathcal{T}_h$ by $\mathcal{E}_K$. $\mathcal{E}_{h,i}^{\mathrm{int}}$ is the set of interior edges (faces) of the subdomain Ω_i, $\mathcal{E}_{h,i}^{\mathrm{ext}} = \mathcal{E}_{h,i}^{\Gamma^{\mathrm{D}}} \cup \mathcal{E}_{h,i}^{\Gamma^{\mathrm{N}}}$ is the set of boundary edges (faces) on $\partial\Omega \cap \partial\Omega_i$, and $\mathcal{E}_h^{\Gamma_{\mathrm{i,j}}}$ is the set of edges (faces) on the interface $\Gamma_{i,j}$. Then $\mathcal{E}_{h,i} = (\bigcup_{j \in B^i} \mathcal{E}_h^{\Gamma_{\mathrm{i,j}}}) \cup \mathcal{E}_{h,i}^{\mathrm{int}} \cup \mathcal{E}_{h,i}^{\mathrm{ext}}$. Let h_K denote the diameter of K and let h_i be the largest diameter of all triangles (tetrahedra if $d = 3$) in $\mathcal{T}_{h,i}$, i.e., $h_i = \max_{K \in \mathcal{T}_{h,i}} h_K$.

2.2 Partitions of the time interval $(0, T)$

Let $\{t^n\}_{0 \leq n \leq N}$ be a sequence of discrete times of the domain Ω as well as of the subdomain Ω_i, $i \in [\![1, \mathcal{N}]\!]$, with $t^0 = 0 < t^1 < \cdots < t^{N-1} < t^N = T$. We consider a partition of the time interval $(0, T)$ into subintervals $I_n := (t^{n-1}, t^n]$ and set $\tau^n := t^n - t^{n-1}$ for all $1 \leq n \leq N$. An extension to subdomains with different time meshes is given in [4].

2.3 Some functions spaces

We define here some basic function spaces. For a given non-empty domain $D \subset \Omega$ and a real number l, $1 \leq l \leq \infty$, we use the standard functional notations $L^l(D)$ and $\mathbf{L}^l(D) := [L^l(D)]^d$ of Lebesgue spaces. We denote by $(\cdot, \cdot)_D$ the scalar product for $L^2(D)$ and $\mathbf{L}^2(D)$, associated with the norm $\|\cdot\|_D$, and by $|D|$ the Lebesgue measure of D. Shall $D = \Omega$, the index will be dropped. Let $\langle \cdot, \cdot \rangle_\gamma$ be the scalar product for the $d-1$ dimensional $L^2(\gamma)$ on $\gamma = \partial D$ or a subset of it. Let also $H^1(D) := \{v \in L^2(D);\ \nabla v \in \mathbf{L}^2(D)\}$ be the Sobolev space of scalar-valued functions with weak derivatives square-integrable and let $\mathbf{H}(\mathrm{div}, D) := \{\mathbf{v} \in \mathbf{L}^2(D);\ \nabla\cdot\mathbf{v} \in L^2(D)\}$ be the space of vector-valued functions whose weak divergences are square-integrable. Finally, for any scalar-, vector-, or tensor-valued function φ defined on Ω, we let φ_i denote the restriction of φ to Ω_i, $i = 1, .., \mathcal{N}$.

3 Global-in-time optimized Schwarz method using OSWR

In this part we present a nonoverlapping space-time domain decomposition method, the optimized Schwarz waveform relaxation (OSWR) method introduced in [26, 37, 10, 11], and studied in [28, 29, 30] in the context of a mixed formulation.

Using the notations of Section 2, the original problem (1.1) can be reformulated as the following equivalent multi-domain problem, for $i \in [\![1, \mathcal{N}]\!]$:

$$\mathbf{u}_i = -\nabla p_i \quad \text{in} \quad \Omega_i \times (0,T), \tag{3.1a}$$

$$\frac{\partial p_i}{\partial t} + \nabla\cdot\mathbf{u}_i = f \quad \text{in} \quad \Omega_i \times (0,T), \tag{3.1b}$$

$$p_i = g_{\mathrm{D}} \quad \text{on} \quad \Gamma_i^{\mathrm{D}} \times (0,T), \tag{3.1c}$$

$$-\mathbf{u}_i\cdot\mathbf{n} = g_{\mathrm{N}} \quad \text{on} \quad \Gamma_i^{\mathrm{N}} \times (0,T), \tag{3.1d}$$

$$p(\cdot,0) = p_0(\cdot) \quad \text{in} \quad \Omega_i, \tag{3.1e}$$

together with the continuity of the potential p and of the normal trace of the flux $\mathbf{u}$ on the space-time interface $\Gamma_{i,j} \times (0,T)$:

$$p_i = p_j \quad \text{and} \quad \mathbf{u}_i\cdot\mathbf{n}_i + \mathbf{u}_j\cdot\mathbf{n}_j = 0 \quad \text{on} \quad \Gamma_{i,j} \times (0,T),\ \forall j \in B^i. \tag{3.2}$$

Alternatively, one may replace the conditions (3.2) by equivalent Robin transmission conditions [35] as follows

$$-\beta_{i,j}\mathbf{u}_i\cdot\mathbf{n}_i + p_i = -\beta_{i,j}\mathbf{u}_j\cdot\mathbf{n}_i + p_j \quad \text{on} \quad \Gamma_{i,j} \times (0,T),\ \forall j \in B^i, \tag{3.3}$$

where $\beta_{i,j} > 0$, $j \in B^i$, $i \in [\![1, \mathcal{N}]\!]$ are free coefficients that may be optimized to improve the convergence factor of the iterative domain decomposition algorithm described below (see [10, 24, 26, 31, 37]).

3.1 The continuous space-time DD algorithm

The optimized Schwarz waveform relaxation (OSWR) algorithm for solving problem (1.1) is defined as follows:
Find the solutions p_i^k and $\mathbf{u}_i^k$ in subdomain Ω_i (in an appropriate mixed formulation), at iteration k, for $k \geq 1$, such that:

$$\mathbf{u}_i^k = -\nabla p_i^k \quad \text{in} \quad \Omega_i \times (0,T), \tag{3.4a}$$

$$\frac{\partial p_i^k}{\partial t} + \nabla\cdot\mathbf{u}_i^k = f \quad \text{in} \quad \Omega_i \times (0,T), \tag{3.4b}$$

$$p_i^k = g_{\mathrm{D}} \quad \text{on} \quad \Gamma_i^{\mathrm{D}} \times (0,T), \tag{3.4c}$$

$$-\mathbf{u}_i^k\cdot\mathbf{n} = g_{\mathrm{N}} \quad \text{on} \quad \Gamma_i^{\mathrm{N}} \times (0,T), \tag{3.4d}$$

$$-\beta_{i,j}\mathbf{u}_i^k\cdot\mathbf{n}_i + p_i^k = g_{\mathrm{R},j}^{k-1} \quad \text{on} \quad \Gamma_{i,j} \times (0,T),\ \forall j \in B^i, \tag{3.4e}$$

$$p(\cdot,0) = p_0 \quad \text{in} \quad \Omega_i, \tag{3.4f}$$

where $g_{\mathrm{R},j}^{k-1} := -\beta_{i,j}\mathbf{u}_j^{k-1}\cdot\mathbf{n}_i + p_j^{k-1}$ for $k \geq 2$ is the information coming from the neighboring subdomain Ω_j, $j \in B^i$, at step k of the algorithm. This algorithm starts from initial guesses $g_{\mathrm{R},j}^0$ which are given functions in $L^2(0,T;L^2(\Gamma_{i,j}))$, $j \in B^i$, $1 \leq i \leq \mathcal{N}$, (see [28] for the convergence analysis and well-posedness).

The OSWR algorithm can be interpreted as a block-Jacobi method applied to a space-time interface problem, see [14, 28, 3, 4] in the context of a mixed formulation. On can replace the block-Jacobi iterations by Krylov-type methods like GMRES (see e.g. [17, 28, 4], and [3] for details). In Sec. 5 below, we will present numerical results both for the block-Jacobi iterations and GMRES.

Note that in the context of mixed finite elements, the potential p_i^k is in $L^2(\Omega_i)$, so that $p_i^k|_{\Gamma_{i,j}}$ is not well defined. Thus a Robin condition $-\beta_{i,j}\mathbf{u}_i^k\cdot\mathbf{n}_i + p_i^k = g_{\mathrm{R},j}^{k-1}$, with a given Robin boundary data $g_{\mathrm{R},j}^{k-1}$ on $\Gamma_{i,j} \times (0,T)$ actually defines the boundary value p_i^k on $\Gamma_{i,j} \times (0,T)$ through the well-defined expression

$$p_i^k|_{\Gamma_{i,j}} := g_{\mathrm{R},j}^{k-1} + \beta_{i,j}\mathbf{u}_i^k\cdot\mathbf{n}_i. \tag{3.5}$$

3.2 The fully discrete space-time DD algorithm

In this part, after introducing some notations for the time and space discretizations, we present the fully discrete counterpart of the OSWR algorithm (3.4), using the lowest-order mixed finite element method (MFE) in space and the discontinuous Galerkin method of order zero in time (DG0) [46] (corresponding to the backward Euler scheme for piecewise-constant-in-time source term f).

3.2.1 Notations for time discretization

Let E be a space of functions defined on a subset D of Ω (e.g. a subdomain or an interface) and let $v(\cdot,t)$ be a function taking its values in E. We denote $P_\tau^0(E)$ the vector space such that $v(\mathbf{x},\cdot)$, $\mathbf{x}\in D$, is piecewise constant in time:

$$P_\tau^0(E) := \{v(\cdot,t) : (0,T)\to E;\ v(\cdot,t) \text{ is constant on } I_n,\ 1\le n\le N\}. \tag{3.6}$$

A function in $P_\tau^0(E)$ is thus defined by the N functions $\{v^n := v(\cdot,t)|_{I_n}\}_{1\le n\le N}$ in E. This allows us to define, for the physical data, $\tilde f_i \in P_\tau^0(L^2(\Omega_i))$, $\tilde g_{\mathrm{D},i}\in P_\tau^0(L^2(\Gamma_i^{\mathrm{D}}))$, and $\tilde g_{\mathrm{N},i}\in P_\tau^0(L^2(\Gamma_i^{\mathrm{N}}))$ such that, for $n=1,..,N$:

$$\tilde f_i|_{I_n} := \tilde f^n,\quad \tilde g_{\mathrm{D},i}|_{I_n} := \tilde g_{\mathrm{D}}^n,\ \text{ and }\ \tilde g_{\mathrm{N},i}|_{I_n} := \tilde g_{\mathrm{N}}^n,\ \ 1\le n\le N, \tag{3.7}$$

where

$$\tilde f^n := \frac{1}{\tau^n}\int_{I_n} f(\cdot,t)\mathrm{d}t,\quad \tilde g_{\mathrm{D}}^n := \frac{1}{\tau^n}\int_{I_n} g_{\mathrm{D}}(\cdot,t)\mathrm{d}t,\quad \tilde g_{\mathrm{N}}^n := \frac{1}{\tau^n}\int_{I_n} g_{\mathrm{N}}(\cdot,t)\mathrm{d}t.$$

In addition, for the a posteriori estimates below, we introduce the following space:

$$\begin{aligned} P_\tau^1(E) := \{&v(\cdot,t) : (0,T)\to E;\ v(\cdot,t)\in C^0(0,T;E),\\ &v(\cdot,t) \text{ is affine on } I_n,\ 1\le n\le N\}. \end{aligned} \tag{3.8}$$

Note that a function in $P_\tau^1(E)$ is defined by $N+1$ functions $\{v^n := v(\cdot,t^n)\}_{0\le n\le N}$, and that if $v\in P_\tau^1(E)$, then $\partial_t v\in P_\tau^0(E)$ is such that

$$\partial_t v|_{I_n} = \frac{1}{\tau^n}(v^n - v^{n-1}),\ 1\le n\le N. \tag{3.9}$$

3.2.2 Notations for space discretization

Let $M_{h,i}\times\mathbf{W}_{h,i}\subset L^2(\Omega_i)\times\mathbf{H}(\mathrm{div},\Omega_i)$ be the Raviart–Thomas–Nédélec mixed finite element spaces of order 0 for Ω_i:

$$M_{h,i} := \{q_{h,i}\in L^2(\Omega_i);\ q_{h,i}|_K\in\mathbb{P}^0(K),\ \forall K\in\mathcal{T}_{h,i}\},$$

where $\mathbb{P}^0(K)$ is the space of polynomials of degree 0, and

$$\mathbf{W}_{h,i} := \{\mathbf{v}_{h,i}\in\mathbf{H}(\mathrm{div},\Omega_i);\ \mathbf{v}_{h,i}|_K\in\mathbf{RTN}_0(K),\ \forall K\in\mathcal{T}_{h,i}\},$$

where $\mathbf{RTN}_0(K) := [\mathbb{P}_0(K)]^d + \mathbf{x}\mathbb{P}_0(K)$, $\mathbf{x}\in\mathbb{R}^d$, is the Raviart–Thomas–Nédélec space of degree zero associated with the element $K\in\mathcal{T}_{h,i}$. We define

$$\begin{aligned} \mathbf{W}_{h,i}^0 &:= \Big\{\mathbf{w}_{h,i}\in\mathbf{W}_{h,i};\ \mathbf{w}_{h,i}\cdot\mathbf{n}|_e = 0\Big\},\quad e\subset\Gamma_i^{\mathrm{N}},\\ \mathbf{W}_{h,i}^{g_{\mathrm{N}},n} &:= \Big\{\mathbf{w}_{h,i}\in\mathbf{W}_{h,i};\ \mathbf{w}_{h,i}\cdot\mathbf{n}|_e = \frac{1}{|e|}\int_e \tilde g_{\mathrm{N}}^{n,i}\mathrm{d}\gamma\Big\},\quad e\subset\Gamma_i^{\mathrm{N}},\ n=1,...,N,\\ \mathbf{W}_{h,i}^{g_{\mathrm{N}}} &:= \{\mathbf{w}_{h\tau,i}\in P_\tau^0(\mathbf{W}_{h,i});\ \mathbf{w}_{h\tau,i}|_{I_n}\in\mathbf{W}_{h,i}^{g_{\mathrm{N}},n}\}, \end{aligned}$$

where $|e|$ is the measure of an edge (face if $d=3$) $e\subset\Gamma_i^{\mathrm{N}}$. In the following, for a subdomain Ω_i, $p_{h\tau,i}$ is a function in $P_\tau^0(M_{h,i})$ such that, on each element $K\in\mathcal{T}_{h,i}$, $p_{h\tau,i}(\cdot,0) = \dfrac{1}{|K|}\displaystyle\int_K p_0\mathrm{d}\mathbf{x}$, and $\mathbf{u}_{h\tau,i}$ is a function in $\mathbf{W}_{h,i}^{g_{\mathrm{N}}}$.

3.2.3 Discrete space-time DD algorithm

The discrete OSWR algorithm at iteration $k \geq 1$ in the subdomain Ω_i, $\forall i \in [\![1, \mathcal{N}]\!]$, is:

Find $\mathbf{u}_{h,i}^{k,n} \in \mathbf{W}_{h,i}^{g_{\mathrm{N}},n}$ and $p_{h,i}^{k,n} \in M_{h,i}$ on I_n, for $n = 1, .., N$, such that:

$$\mathbf{a}_i(\mathbf{u}_{h,i}^{k,n}, \mathbf{v}_{h,i}) - \mathbf{b}_i(\mathbf{v}_{h,i}, p_{h,i}^{k,n}) = \boldsymbol{\ell}_i^{k-1,n}(\mathbf{v}_{h,i}), \quad \forall \mathbf{v}_{h,i} \in \mathbf{W}_{h,i}^0, \tag{3.10a}$$

$$\frac{1}{\tau^n}(p_{h,i}^{k,n} - p_{h,i}^{k,n-1}, q_{h,i})_{\Omega_i} + \mathbf{b}_i(\mathbf{u}_{h,i}^{k,n}, q_{h,i}) = (\tilde{f}^n, q_{h,i})_{\Omega_i}, \quad \forall q_{h,i} \in M_{h,i}, \tag{3.10b}$$

$$(p_{h,i}^{k,0}, q_{h,i})_{\Omega_i} = (p_0, q_{h,i})_{\Omega_i}, \quad \forall q_{h,i} \in M_{h,i}, \tag{3.10c}$$

where the bilinear forms $\mathbf{a}_i$ and $\mathbf{b}_i$, and the linear form $\boldsymbol{\ell}_i^{k,n}$, $k \geq 0$, are defined by:

$$\begin{aligned}
&\mathbf{a}_i : \mathbf{W}_{h,i} \times \mathbf{W}_{h,i} \to \mathbb{R},\ \mathbf{a}_i(\mathbf{u}_{h,i}, \mathbf{v}_{h,i}) := (\mathbf{u}_{h,i}, \mathbf{v}_{h,i})_{\Omega_i} + \sum_{j \in B^i} \langle \beta_{i,j} \mathbf{u}_{h,i} \cdot \mathbf{n}_i, \mathbf{v}_{h,i} \cdot \mathbf{n}_i \rangle_{\Gamma_{i,j}},\\
&\mathbf{b}_i : \mathbf{W}_{h,i} \times M_{h,i} \to \mathbb{R},\ \mathbf{b}_i(\mathbf{v}_{h,i}, q_{h,i}) := (q_{h,i}, \nabla \cdot \mathbf{v}_{h,i})_{\Omega_i},\\
&\boldsymbol{\ell}_i^{k,n} : \quad \mathbf{W}_{h,i} \to \mathbb{R}, \quad \boldsymbol{\ell}_i^{k,n}(\mathbf{v}_{h,i}) := -\langle \tilde{g}_{\mathrm{D}}^{n,i}, \mathbf{v}_{h,i} \cdot \mathbf{n}_i \rangle_{\Gamma_i^{\mathrm{D}}} - \sum_{j \in B^i} \langle \tilde{g}_{\mathrm{R},j}^{k,n}, \mathbf{v}_{h,i} \cdot \mathbf{n}_i \rangle_{\Gamma_{i,j}},
\end{aligned}$$

where

$$\tilde{g}_{\mathrm{R},j}^{k,n} := \frac{1}{\tau^n} \int_{I_n} g_{\mathrm{R},j}^k(\cdot, t)\, \mathrm{d}t. \tag{3.11}$$

Here, $\tilde{g}_{\mathrm{R},j}^{0,n}$ is a given initial guess on $\Gamma_{i,j}$ and, using (3.5), $\langle \tilde{g}_{\mathrm{R},j}^{k,n}, \boldsymbol{\psi}_{e'} \cdot \mathbf{n}_i \rangle_{\Gamma_{i,j}}$, for $k \geq 1$ and the basis function $\boldsymbol{\psi}_{e'}$ on $e' \in \Gamma_{i,j}$, is given by:

$$\langle \tilde{g}_{\mathrm{R},j}^{k,n}, \boldsymbol{\psi}_{e'} \cdot \mathbf{n}_i \rangle_{\Gamma_{i,j}} = \int_{\Gamma_{i,j}} \beta_{i,j} (\mathbf{u}_{h,j}^{k,n} \cdot \mathbf{n}_j) \boldsymbol{\psi}_{e'} \cdot \mathbf{n}_i \, \mathrm{d}\gamma + \int_{\Gamma_{i,j}} (\beta_{j,i} \mathbf{u}_{h,j}^{k,n} \cdot \mathbf{n}_j + \tilde{g}_{\mathrm{R},i}^{k-1,n}) \mathrm{d}\gamma, \tag{3.12}$$

and is equal to zero when $e' \notin \Gamma_{i,j}$.

Remark 3.1 *Note that using the rectangle quadrature rule, $\tilde{f}^n$, $\tilde{g}_{\mathrm{D}}^n$, and $\tilde{g}_{h,\mathrm{N}}^n$ can be approximated by:*

$$\tilde{f}^n \approx f(\cdot, t^n), \quad \tilde{g}_{\mathrm{D}}^n \approx g_{\mathrm{D}}(\cdot, t^n), \quad \tilde{g}_{h,\mathrm{N}}^n \approx g_{h,\mathrm{N}}(\cdot, t^n), \quad \tilde{g}_{\mathrm{R},j}^{k,n} \approx g_{\mathrm{R},j}^k(\cdot, t^n),$$

so that the DG0 method in time is equivalent to the backward Euler scheme.

4 A posteriori error estimate: fully computable upper bound

The objective of this section is to bound the error between the exact solution and the approximate solution at each iteration k of the space-time DD method, by indicators that are completely calculable and constructed from the approximate solution $(p_{h\tau}^k, \mathbf{u}_{h\tau}^k)$.

For simplicity, let $\Gamma^{\mathrm{N}} = \emptyset$ and $g_{\mathrm{D}} = 0$ (exstension of the results to the general case can be done following e.g., [18, 19, 16] and the references therein). We use for the error the space-time energy norm given in [47, 19, 20]. A postprocessing $\tilde{p}_{h\tau}^k$ is first constructed, from which we build a subdomain potential reconstruction $\bar{s}_{h\tau,i}^k$ for each subdomain Ω_i, $\forall i \in [\![1, \mathcal{N}]\!]$, on each iteration of the space-time DD algorithm, following [3], so as to distinguish the error from $H_0^1(\Omega)$-nonconformity and from domain decomposition. From $\tilde{p}_{h\tau}^k$ and following [20], we also build a potential reconstruction $s_{h\tau}^k$ on each space-time DD iteration. Then, to evaluate the error in the $\mathbf{H}(\mathrm{div}, \Omega)$-nonconformity, we build a flux reconstruction $\boldsymbol{\sigma}_{h\tau}^k$ on each iteration of the space-time DD algorithm, using the same idea of extracting bands and solving local Neumann problems as proposed in [3]. Details of concrete candidates for these reconstructions are given in [4]. This allows to distinguish the space discretization error, the time discretization error, and the domain decomposition error.

Let us first introduce the broken Sobolev space

$$H^1(\mathcal{T}_h) := \{v \in L^2(\Omega);\, v|_K \in H^1(K),\ \forall K \in \mathcal{T}_h\}$$

and the energy semi-norm on $H^1(\mathcal{T}_h)$, defined for all $\varphi \in H^1(\mathcal{T}_h)$ by

$$|||\varphi|||^2 := \sum_{K\in\mathcal{T}_h} |||\varphi|||_K^2 := \sum_{K\in\mathcal{T}_h} \|\nabla\varphi\|_K^2,$$

as well as the energy norm on $\mathbf{L}^2(\Omega)$, defined for all $\mathbf{v} \in \mathbf{L}^2(\Omega)$ by

$$|||\mathbf{v}|||_\star^2 := \sum_{K\in\mathcal{T}_h} |||\mathbf{v}|||_{\star,K}^2 := \sum_{K\in\mathcal{T}_h} \|\mathbf{v}\|_K^2.$$

For a given function v, its jump and average are then defined respectively as:

$$\begin{cases} [\![v]\!] := v|_K - v|_{K'} \text{ and } \{\!\{v\}\!\} := \dfrac{1}{2}(v|_K + v|_{K'}) & \text{if } e \in \Big(\underset{j\in B^i}{\cup} \mathcal{E}_h^{\Gamma_{i,j}}\Big) \cup \mathcal{E}_{h,i}^{\text{int}}, \\ [\![v]\!] := v|_e - g_{\text{D}} \text{ and } \{\!\{v\}\!\} := \dfrac{1}{2}(v|_e + g_{\text{D}}) & \text{if } e \in \mathcal{E}_{h,i}^{\Gamma^{\text{D}}}. \end{cases}$$

We recall, for the forthcoming theorems, the Poincaré inequality: for $K \in \mathcal{T}_h$, since K is convex,

$$\|\varphi - \pi_0\varphi\|_K \le \frac{h_K}{\pi}\|\nabla\varphi\|_K \qquad \forall\varphi \in H^1(K), \tag{4.1}$$

where $\pi_0\varphi$ is the mean value of φ on K.

4.1 Postprocessing of the approximate solution

Following the work in [8, 5, 48], we first construct a postprocessing $\tilde{p}_{h,i}^{k,n} \in \mathbb{P}_2(\mathcal{T}_{h,i})$ of $p_{h,i}^{k,n}$, for each subdomain $i \in [\![1,\mathcal{N}]\!]$, at each iteration $k \ge 1$ of the space-time DD algorithm, on each time step n, $1 \le n \le N$, as follows:

$$-\nabla\tilde{p}_{h,i}^{k,n}|_K = \mathbf{u}_{h,i}^{k,n}|_K, \qquad \forall K \in \mathcal{T}_{h,i}, \tag{4.2a}$$

$$\pi_0(\tilde{p}_{h,i}^{k,n}|_K) = p_{h,i}^{k,n}|_K, \qquad \forall K \in \mathcal{T}_{h,i}, \tag{4.2b}$$

and we define $\tilde{p}_h^{k,n}|_{\Omega_i} = \tilde{p}_{h,i}^{k,n}$. Then, the postprocessing of the approximate solution for which the a posteriori error analysis will be done in Sec. 4.3 is defined as follows:

$$\tilde{p}_{h\tau}^k \in P_\tau^1(\mathbb{P}_2(\mathcal{T}_h)), \quad \tilde{p}_{h\tau}^k(\cdot,t^n) := \tilde{p}_h^{k,n}.$$

4.2 Concept of of potential and flux reconstructions

The main tools of our estimation in Theorem 4.4 are the three supplementary objects $s_{h\tau}^k$, $\overline{s}_{h\tau}^k$, and $\boldsymbol{\sigma}_{h\tau}^k$ defined below, on each iteration $k \ge 1$ of the space-time DD algorithm.

Definition 4.1 (Subdomain potential reconstruction) *We will call a* subdomain potential reconstruction*, for Ω_i, $i \in [\![1,\mathcal{N}]\!]$, any function $\overline{s}_{h\tau,i}^k$ built from $\tilde{p}_{h\tau,i}^k$ such that*

- *it is subdomain $H^1(\Omega_i)$-conforming in space, continuous and piecewise affine in time, i.e.,*

$$\overline{s}_{h\tau,i}^k \in P_\tau^1(H^1(\Omega_i) \cap C^0(\overline{\Omega}_i)), \tag{4.3a}$$

$$\overline{s}_{h\tau,i}^k|_{\Gamma_i^{\text{D}}} = g_{\text{D}}|_{\Gamma_i^{\text{D}}}; \tag{4.3b}$$

- *on each time step n, $0 \le n \le N$, the mean values of $\tilde{p}_{h,i}^{k,n}$ are preserved,*

$$(\overline{s}_{h,i}^{k,n}, 1)_K = (\tilde{p}_{h,i}^{k,n}, 1)_K, \ \ \forall K \in \mathcal{T}_{h,i}, \tag{4.4}$$

where $\overline{s}_{h,i}^{k,n} := \overline{s}_{h\tau,i}^k(\cdot,t^n)$;

- *it is built locally subdomain by subdomain to capture the nonconformity from the numerical scheme by comparing it with* $\tilde{p}_{h\tau}^k$ *in the sense that the estimators* (4.14d)*, and* (4.14g)*, as well as* (4.14b) *below, (recall* (4.2a) *which explains the comparison of* $-\nabla\overline{s}_h^{k,n}$ *and* $\mathbf{u}_h^{k,n}$*) are as small as possible.*

Definition 4.2 (Potential reconstruction) *We will call a* potential reconstruction *any function* $s_{h\tau}^k$ *constructed from* $\tilde{p}_{h\tau}^k$ *such that*

- *it is globally* $H^1(\Omega)$*-conforming in space, continuous and piecewise affine in time, i.e.,*

$$s_{h\tau}^k \in P_\tau^1(H^1(\Omega)\cap C^0(\overline{\Omega})), \tag{4.5a}$$

$$s_{h\tau}^k|_{\Gamma^{\mathrm{D}}} = g_{\mathrm{D}}, \tag{4.5b}$$

- *on each time step* n*,* $0\le n\le N$*, the mean values of* $\tilde{p}_h^{k,n}$ *are preserved,*

$$(s_h^{k,n},1)_K = (\tilde{p}_h^{k,n},1)_K,\ \ \forall K\in\mathcal{T}_h, \tag{4.6}$$

where $s_h^{k,n} := s_{h\tau}^k(\cdot,t^n)$*;*

- *its comparison with* $\overline{s}_{h\tau}^k$ *estimates the domain decomposition error in the sense that* $\Big\{\int_0^T |||\overline{s}_{h\tau}^k - s_{h\tau}^k|||^2\mathrm{d}t\Big\}^{\frac12}\to 0$ *and* $\Big\{\int_0^T ||\partial_t(\overline{s}_{h\tau}^k - s_{h\tau}^k)||^2\mathrm{d}t\Big\}^{\frac12}\to 0$ *when* $k\to\infty$*.*

Definition 4.3 (Equilibrated flux reconstruction) *We will call an* equilibrated flux reconstruction *any function* $\boldsymbol{\sigma}_{h\tau}^k$ *constructed from* $\tilde{p}_{h\tau}^k$*,* $\mathbf{u}_{h\tau}^k$*, such that*

- *it is* $\mathbf{H}(\mathrm{div})$*-conforming and locally conservative in space, piecewise constant in time, i.e.,*

$$\boldsymbol{\sigma}_{h\tau}^k \in P_\tau^0(\mathbf{H}(\mathrm{div},\Omega)); \tag{4.7}$$

- *it has a local conservation property on each time step* n*,* $0\le n\le N$*:*

$$(\tilde{f^n} - \partial_t\tilde{p}_{h\tau}^k|_{I_n} - \nabla\cdot\boldsymbol{\sigma}_h^{k,n},1)_K = 0,\ \ \forall K\in\mathcal{T}_h, \tag{4.8}$$

together with the Neumann condition:

$$-(\boldsymbol{\sigma}_h^{k,n}\cdot\mathbf{n}_\Omega,1)_e = (\tilde{g}_{\mathrm{N}},1)_e, \qquad \forall e\in\bigcup_{i=1}^{\mathcal{N}}\mathcal{E}_{h,i}^{\Gamma^{\mathrm{N}}}, \tag{4.9}$$

where $\boldsymbol{\sigma}_h^{k,n} := \boldsymbol{\sigma}_{h\tau}^k|_{I_n}$*;*

- *its comparison with* $\mathbf{u}_{h\tau}^k$ *is used to estimate the space-time DD error in the sense that* $\Big\{\int_0^T |||\mathbf{u}_{h\tau}^k - \boldsymbol{\sigma}_{h\tau}^k|||_\star^2\mathrm{d}t\Big\}^{\frac12}\to 0$ *when* $k\to\infty$*.*

4.3 General a posteriori error estimate: fully computable upper bound

Let $X := L^2(0,T;H_0^1(\Omega))$ and $X' = L^2(0,T;H^{-1}(\Omega))$; The nonconforming approximation $\tilde{p}_{h\tau}^k$ of Section 4.1, leads to introduce the following broken X-norm where ∇ is the broken gradient operator:

$$|||q|||_X^2 := \sum_{n=1}^N\int_{I_n}||\nabla q(\cdot,t)||^2\mathrm{d}t = \sum_{n=1}^N\int_{I_n}\sum_{K\in\mathcal{T}_h}||\nabla q(\cdot,t)||_K^2\,\mathrm{d}t.$$

Let $Y := \{q\in X;\partial_t q\in X'\}$, endowed we with the space-time norm of [19]:

$$|||q|||_Y^2 := |||q|||_X^2 + ||\partial_t q||_{X'}^2 + ||q(\cdot,T)||^2, \tag{4.10}$$

where

$$||\partial_t q||_{X'} := \left\{ \int_0^T ||\partial_t q||^2_{H^{-1}(\Omega)} \,\mathrm{d}t \right\}^{\frac{1}{2}} := \left\{ \int_0^T \left(\sup_{v \in H^1_0(\Omega);\, \|\nabla v\|=1} \langle \partial_t q, v \rangle \right)^2 \mathrm{d}t \right\}^{\frac{1}{2}}.$$

The Y- and X'-norms are again extended to piecewise regular-in-space functions, since $\tilde{p}_{h\tau} \notin X$. By the weak solution of problem (1.1) under the above assumptions, we then understand $p \in Y$ such that $p(\cdot,0) = p_0$ and

$$\int_0^T \{\langle \partial_t p, v\rangle + (\nabla p, \nabla v)\} \,\mathrm{d}t = \int_0^T (f,v) \,\mathrm{d}t \qquad \forall v \in X. \tag{4.11}$$

Our main result is then:

Theorem 4.4 (A posteriori error estimates for the potential, distinguishing space, time, and domain decor
Let p be the weak solution of problem (1.1) *given by* (4.11)*. Let $\tilde{p}^k_{h\tau} \in P^1_\tau(H^1(\mathcal{T}_h))$ be an arbitrary approximation to p; in particular $\tilde{p}^{k,n}_h = \tilde{p}^k_{h\tau}(\cdot,t^n)$ can be the postprocessing* (4.2) *of the solution $(p^{k,n}_h, \mathbf{u}^{k,n}_h)$ at iteration k of the global-in-time optimized Schwarz algorithm* (3.10)–(3.12)*. Let $\mathbf{u}^{k,n}_h|_K := -\nabla \tilde{p}^{k,n}_h|_K$ in each element $K \in \mathcal{T}_h$. Let $\overline{s}^k_{h\tau,i}$ be the subdomain potential reconstruction of Definition 4.1, let $s^k_{h\tau}$ be the potential reconstruction of Definition 4.2, and let $\boldsymbol{\sigma}^k_{h\tau}$ be the equilibrated flux reconstruction of Definition 4.3. Then there holds*

$$|||p - \tilde{p}^k_{h\tau}|||_Y \le \tilde{\eta}^k := \eta^k_{\mathrm{sp}} + \eta^k_{\mathrm{tm}} + \eta^k_{\mathrm{DD}} + \eta^k_{\mathrm{IC}} + ||f - \tilde{f}||_{X'}, \tag{4.12}$$

where the "spatial discretization estimator" is

$$\begin{aligned}\eta^k_{\mathrm{sp}} :=& \left\{ \sum_{n=1}^N \tau^n \sum_{K\in\mathcal{T}_h} (\eta^{k,n}_{\mathrm{osc},K} + \eta^{k,n}_{\mathrm{DF},1,a,K})^2 \right\}^{\frac{1}{2}} + \left\{ \sum_{n=1}^N \int_{I_n} \sum_{K\in\mathcal{T}_h} (\eta^k_{\mathrm{NCP},1,a,K}(t))^2 \mathrm{d}t \right\}^{\frac{1}{2}} \\ &+ \left\{ \sum_{n=1}^N \tau^n \sum_{K\in\mathcal{T}_h} (\eta^{k,n}_{\mathrm{NCP},2,a,K})^2 \right\}^{\frac{1}{2}} + ||s^{k,N}_h - \tilde{p}^{k,N}_h||,\end{aligned}$$

the "time discretization estimator" is

$$\eta^k_{\mathrm{tm}} := \left\{ \sum_{n=1}^N \sum_{K\in\mathcal{T}_h} \frac{1}{3}\tau^n |||s^{k,n}_h - s^{k,n-1}_h|||^2_K \right\}^{\frac{1}{2}},$$

the "domain decomposition estimator" is

$$\begin{aligned}\eta^k_{\mathrm{DD}} :=& \left\{ \sum_{n=1}^N \tau^n \sum_{K\in\mathcal{T}_h} (\eta^{k,n}_{\mathrm{DF},1,b,K} + \eta^{k,n}_{\mathrm{NCP},1,b,K})^2 \right\}^{\frac{1}{2}} \\ &+ \left\{ \sum_{n=1}^N \int_{I_n} \sum_{K\in\mathcal{T}_h} (\eta^k_{\mathrm{NCP},1,b,K}(t))^2 \mathrm{d}t \right\}^{\frac{1}{2}} \\ &+ \left\{ \sum_{n=1}^N \tau^n \sum_{K\in\mathcal{T}_h} (\eta^{k,n}_{\mathrm{NCP},2,b,K})^2 \right\}^{\frac{1}{2}},\end{aligned} \tag{4.13}$$

and the "initial condition estimator" is

$$\eta^k_{\mathrm{IC}} := ||s^{k,0}_h - p_0||.$$

For all $1 \le n \le N$ *and* $K \in \mathcal{T}_h$*, the following terms are the elementwise estimators:*

$$\eta_{\mathrm{osc},K}^{k,n} := \frac{h_K}{\pi} \|\tilde{f}^n - \partial_t s_{h\tau}^k|_{I_n} - \nabla\cdot\boldsymbol{\sigma}_h^{k,n}\|_K \quad \textit{"data oscillation"}, \tag{4.14a}$$

$$\eta_{\mathrm{DF},1,a,K}^{k,n} := |||\nabla \overline{s}_h^{k,n} + \mathbf{u}_h^{k,n}|||_{\star,K}, \quad \textit{"constitutive relation"}, \tag{4.14b}$$

$$\eta_{\mathrm{DF},1,b,K}^{k,n} := |||\mathbf{u}_h^{k,n} - \boldsymbol{\sigma}_h^{k,n}|||_{\star,K}, \quad \textit{"DD flux nonconformity"}, \tag{4.14c}$$

$$\eta_{\mathrm{NCP},1,a,K}^{k}(t) := |||(\tilde{p}_{h\tau}^k - \overline{s}_{h\tau}^k)(t)|||_K, \ \ t \in I_n \quad \textit{"potential nonconformity"}, \tag{4.14d}$$

$$\eta_{\mathrm{NCP},1,b,K}^{k}(t) := |||(\overline{s}_{h\tau}^k - s_{h\tau}^k)(t)|||_K, \ \ t \in I_n \quad \textit{"DD potential nonconformity"}, \tag{4.14e}$$

$$\eta_{\mathrm{NCP},1,b,K}^{k,n} := |||\overline{s}_h^{k,n} - s_h^{k,n}|||_K, \ \textit{"DD potential nonconformity"}, \tag{4.14f}$$

$$\eta_{\mathrm{NCP},2,a,K}^{k,n} := \frac{h_K}{\pi} ||\partial_t(\tilde{p}_{h\tau}^k - \overline{s}_{h\tau}^k)|_{I_n}||_K, \ \textit{"potential nonconformity"}, \tag{4.14g}$$

$$\eta_{\mathrm{NCP},2,b,K}^{k,n} := \frac{h_K}{\pi} ||\partial_t(\overline{s}_{h\tau}^k - s_{h\tau}^k)|_{I_n}||_K, \ \textit{"DD potential nonconformity"}. \tag{4.14h}$$

Remark 4.5 *The estimator* η_{DD}^k *is the error due to the global-in-time domain decomposition method and vanishes at the convergence of the DD algorithm.*

5 Numerical results

In this section, we present some numerical illustrations of the a posteriori error estimators of Theorem 4.4.

Let $\Omega =]0,1[\times]0,1[$. In order to illustrate our estimates, we consider the problem (1.1) with solution $p(\mathbf{x},t) = \sin(2\pi x)\sin(2\pi y)\cos(2\pi t)$. The corresponding source term is $f(\mathbf{x},t) = 8\pi^2 \sin(2\pi x)\sin(2\pi y)\cos(2\pi t) - 2\pi \sin(2\pi x)\sin(2\pi y)\sin(2\pi t)$, and we set homogeneous Dirichlet conditions on the top and the bottom of Ω, and Neumann conditions on the other sides of $\partial\Omega$ with $g_N(y,t) = 2\pi \sin(2\pi y)\cos(2\pi t)$.

As noticed in Sec. 3.2, the OSWR algorithm (3.10)–(3.12) can be interpreted as a block-Jacobi method applied to a space-time interface problem, and it can be replaced by GMRES. Numerical results will be shown below, both for block-Jacobi and GMRES.

5.1 Heat equation with the block-Jacobi (OSWR) solver

Number of triangles in Ω	76888
Number of subdomains	9
Subdomain solver	Direct
DD solver	block-Jacobi
Final time	$T = 1$
Time step τ	$1/100$
Original DD stopping criterion	1e-6
A posteriori stopping criterion	$\eta_{\mathrm{DD}} \le 0.1 \max(\eta_{\mathrm{tm}}, \eta_{\mathrm{sp}})$
Total number of iterations	63
Number of iterations with an a posteriori stopping criterion	18
Unnecessary iterations	45
Spared iteration from the total number of iteration	≈ 71 %

Table 1: Example with the block-Jacobi (OSWR) solver

Table 1 summarizes the discretization data as well as the stopping criterion for the DD solver.

Figure 1 presents the evolution of η_{DD} in green, η_{sp} in black, and η_{tm} in magenta, and their sum in blue as a function of the number of iterations of the DD block-Jacobi (OSWR) solver. We remark that η_{DD} dominates until iteration 10 and then gets smaller compared to η_{sp} and η_{tm}. Concerning η_{sp} and η_{tm}, they are constant after iteration 15 and until iteration 63. We have chosen the a posteriori stopping criterion $\eta_{\mathrm{DD}} \le 0.1 \max(\eta_{\mathrm{tm}}, \eta_{\mathrm{sp}})$, leading to 18 iterations, in contrast to the usual stopping criterion, when the

jump of the Robin condition on the interface is less than some fixed tolerance, in our case 10^{-6}, satisfied at iteration 63 only. Figure 1 also shows the evolution of the DD error $|||\tilde{p}_{h\tau}^k - \tilde{p}_{h\tau}^\infty|||_Y$ in cyan, where $\tilde{p}_{h\tau}^\infty$ is the postprocessing of the converged DD solution (computed with a tolerance of 10^{-13}). We observe that $\eta_{\rm DD}$ is also an upper bound of the DD error.

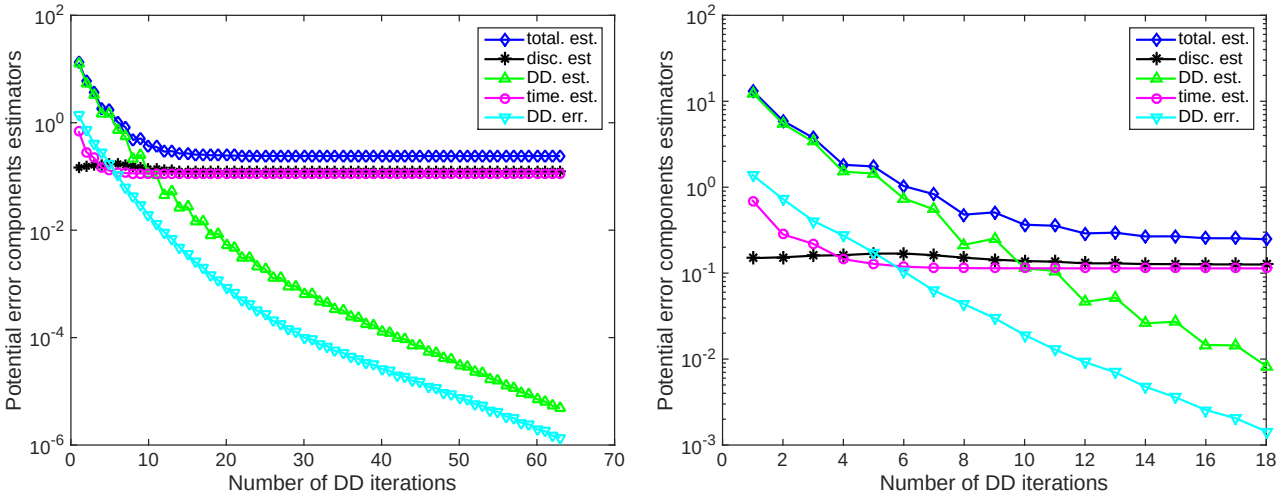

Figure 1: Error component estimates (left), with a zoom until iteration 18 (right), with the block-Jacobi (OSWR) solver

Figure 2 (left) shows the total estimator in red, and a rough approximation of the error $|||p - \tilde{p}_{h\tau}^k|||_Y$ in blue, which is represented here by $\{|||p - \tilde{p}_{h\tau}^k|||_X^2 + ||(p - \tilde{p}_{h\tau}^k)(\cdot, T)||^2\}^{\frac{1}{2}}$ without the term $||\partial_t(p - \tilde{p}_{h\tau}^k)||_{X'}$ whose computation would be difficult to compute, versus the number of iterations k. Consequently, we obtain the effectivity index $I_{\rm eff}^k := \dfrac{\tilde{\eta}^k}{|||p - \tilde{p}_h^k|||_Y}$ from (4.12) defined as the ratio of the estimated and the actual error at the iteration k of the space-time DD algorithm, as shown in Figure 2 on the right. We observe that the effectivity index approaches the value of approximately 6.87. It is not close to the optimal value of 1, one of the reasons may be that the negative norms in Theorem 4.4 have not been computed here.

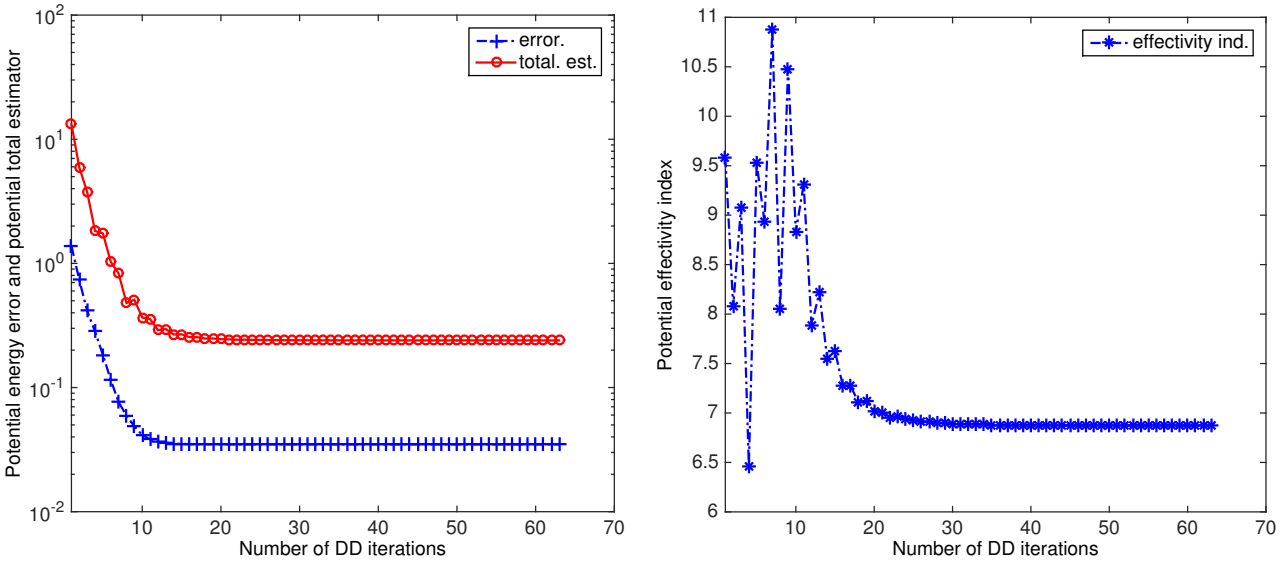

Figure 2: Energy error and total estimator (left), and effectivity index (right), with the block-Jacobi (OSWR) solver

5.1.1 DD estimators at iteration 18

Figure 3 shows the elementwise contributions of the estimators (built using the subdomain potential reconstruction on the interface)

$$\Big\{ \int_{I_{100}} (\eta^{18}_{\mathrm{NCP},1,b,K})^2(t)\,\mathrm{d}t \Big\}^{\frac{1}{2}}, \quad \text{(Figure 3 on the left)},$$

and

$$\Big\{ \tau^{100} (\eta^{18,100}_{\mathrm{NCP},2,b,K})^2 \Big\}^{\frac{1}{2}}, \quad \text{(Figure 3 on the right)}.$$

at the final time $T = 1$, at iteration 18 of the space-time DD algorithm. We remark that the contributions of the elements of $\eta^{18}_{\mathrm{NCP},1,b,K}$ on I_{100} are (in the infinity norm) about $1.2\,10^{-4}$ and distributed around the interfaces of the 9 subdomains, whereas $\eta^{18,100}_{\mathrm{NCP},2,b,K}$ are about $5\,10^{-10}$ around the interfaces. Figure 4 (left),

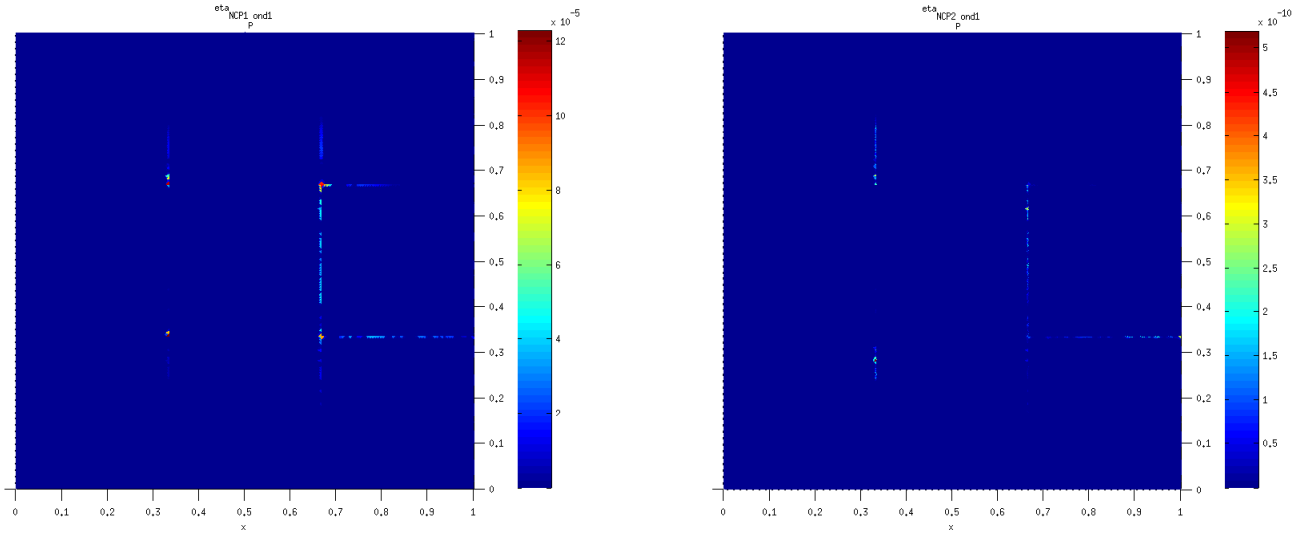

Figure 3: Distribution of $\Big\{ \int_{I_{100}} (\eta^{18}_{\mathrm{NCP},1,b,K})^2(t)\,\mathrm{d}t \Big\}^{\frac{1}{2}}$ on Ω (left) and of $\Big\{ \tau^{100} (\eta^{18,100}_{\mathrm{NCP},2,b,K})^2 \Big\}^{\frac{1}{2}}$ (right) at the final time $T = 1$ and at iteration 18 of the block-Jacobi (OSWR) solver

shows the elementwise contributions of the estimators (built using the subdomain flux reconstruction coming from the local Neumann problems)

$$\Big\{ \tau^{100} (\eta^{18,100}_{\mathrm{DF},1,b,K})^2 \Big\}^{\frac{1}{2}}.$$

We observe that the errors (in the infinity norm) are distributed around the interfaces and are about $2.5\,10^{-5}$. Finally, Figure 4 (right) shows the elementwise contributions of $\eta^{18,100}_{\mathrm{DD}}$, defined as the sum of the three above estimators. It follows the same distribution as $\Big\{ \int_{I_{100}} (\eta^{18}_{\mathrm{NCP},1,b,K})^2(t)\,\mathrm{d}t \Big\}^{\frac{1}{2}}$ that has the largest contribution to $\eta^{18,100}_{\mathrm{DD}}$.

5.1.2 Total discretization estimator, time and global estimators at iteration 18

Figure 5 presents the elementwise contributions of the time discretization estimator $\eta^{18,100}_{\mathrm{tm}}$ (left), which is about 5e-6, and the subdomain discretization estimator $\eta^{18,100}_{\mathrm{sp}}$ (right), which is about 2e-4. We remark that $\eta^{18,100}_{\mathrm{sp}}$ dominates and is close to the total estimator represented in Figure 6 (left), that bound the norm $|||p - \tilde{p}^{18,100}_h|||_Y$ in (4.12) at time step 100. Finally, Figure 6 (on the right) shows the error between the exact solution and the approximate solution $\{|||p - \tilde{p}^{18}_{h\tau}|||^2_X + ||(p - \tilde{p}^{18}_{h\tau})(\cdot, T)||^2\}^{\frac{1}{2}}$ at time step 100. We first

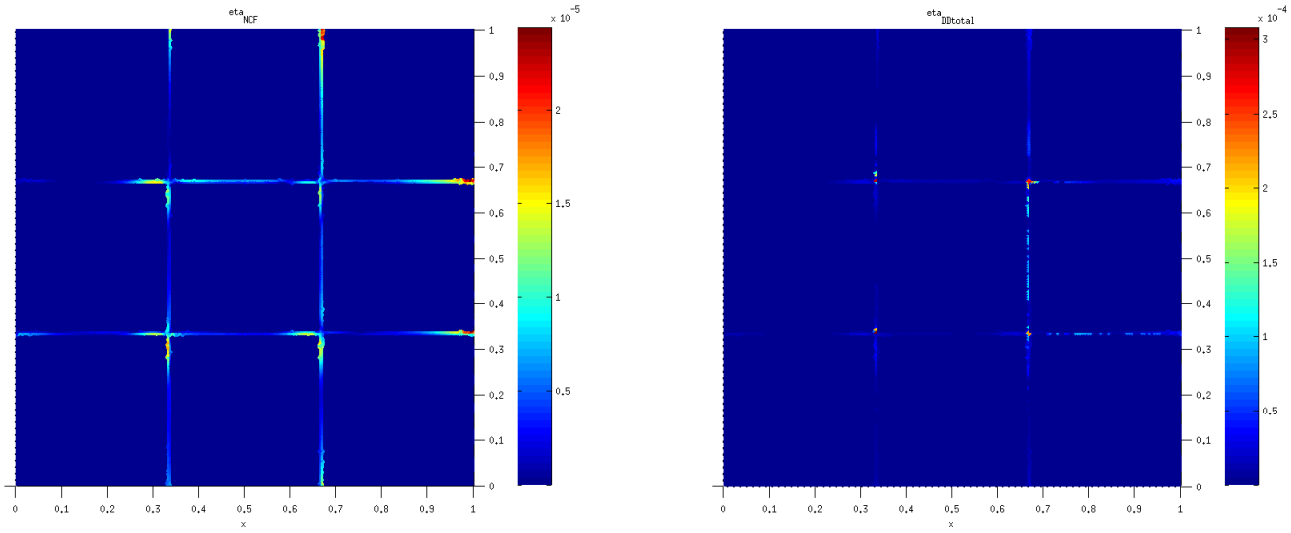

Figure 4: Distribution of the estimator $\left\{\tau^{100}(\eta^{18,100}_{\mathrm{DF},1,b,K})^2\right\}^{\frac{1}{2}}$ on Ω (on the left) and of $\eta^{18,100}_{\mathrm{DD}}$ (on the right) at the final time step 100 and at the 18th iteration of the block-Jacobi (OSWR) solver

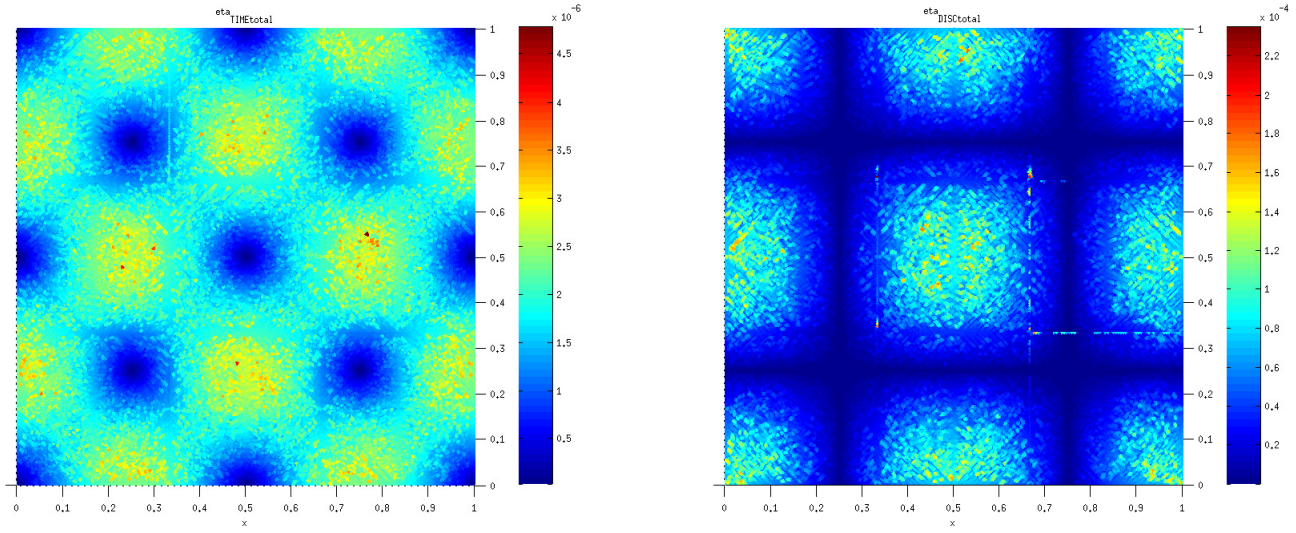

Figure 5: Distribution of the estimator $\eta^{18,100}_{\mathrm{tm}}$ on Ω (on the left) and of $\eta^{18,100}_{\mathrm{sp}}$ (on the right) at the final time step 100 and at the 18th iteration of the block-Jacobi (OSWR) solver

observe that it is about 9.5e-5, and thus smaller than the total estimator in Figure 6 (left), which is about 3.5e-4. The element contributions do not perfectly match with the total estimator, which may be due to the fact that the error $||\partial_t(p-\tilde{p}^{k+1}_{h\tau})||_{X'}$ in $|||p-\tilde{p}^{k+1}_{h\tau}|||_Y$ has not been computed here.

5.2 Model example with the GMRES solver

We consider here the same example as in Section 5.1 but using the GMRES solver, see Table 2. Note that the GMRES solver converges faster than the block-Jacobi solver, as shown in Figure 7. We remark that η_{DD} dominates up to roughly 7 iterations and then gets smaller compared to the discretization and time estimators. Here, we can stop the space-time DD algorithm at iteration 13 when $\eta_{\mathrm{DD}} \leq 0.1 \max(\eta_{\mathrm{tm}}, \eta_{\mathrm{sp}})$,

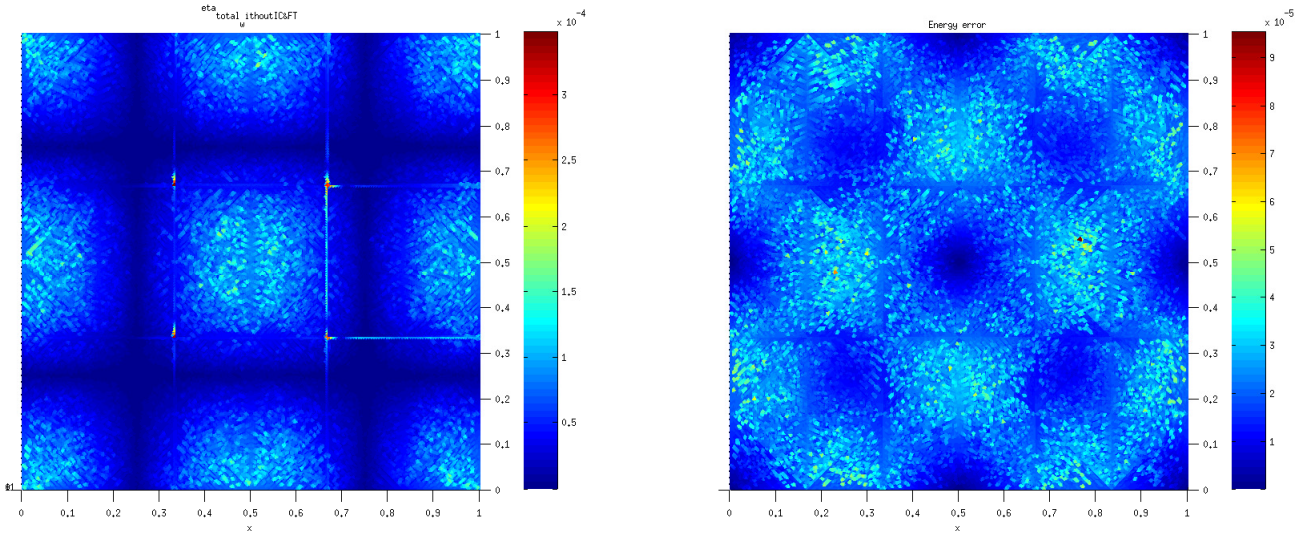

Figure 6: Distribution of the total estimator on Ω (on the left) and of the error between the exact solution and the approximate solution (on the right) at the final time step 100 and at the 18th iteration of the block-Jacobi (OSWR) solver

Number of triangles in Ω	76888
Number of subdomains	9
Subdomain solver	Direct
DD solver	GMRES
Final time	$T = 1$
Time step τ	$1/100$
Original DD stopping criterion	1e-6
A posteriori stopping criterion	$\eta_{\mathrm{DD}} \leq 0.1 \max(\eta_{\mathrm{tm}}, \eta_{\mathrm{sp}})$
Total number of iterations	41
Number of iterations with an a posteriori stopping criterion	13
Unnecessary iterations	28
Spared iteration from the total number of iteration	≈ 68 %

Table 2: Example with the GMRES solver

and thereby avoid 28 unnecessary iterations, and save another 5 iterations compared to the block-Jacobi solver (which stopped at iteration 18). Figure 8 (left) shows the energy error in blue, and the total estimator in red, versus the number of iterations. The effectivity index is represented in Figure 8 (right) and reaches approximately the value 6.8 at the iteration 41 wheras its value is about 7.1 at iteration 13.

References

[1] E. Ahmed, S. Ali Hassan, C. Japhet, M. Kern, and M. Vohralík. A posteriori error estimates and stopping criteria for space-time domain decomposition for two-phase flow between different rock types. HAL Preprint 01540956, submitted for publication, June 2017.

[2] M. Ainsworth. A posteriori error estimation for lowest order Raviart–Thomas mixed finite elements. *SIAM J. Sci. Comput.*, 30(1):189–204, 2007.

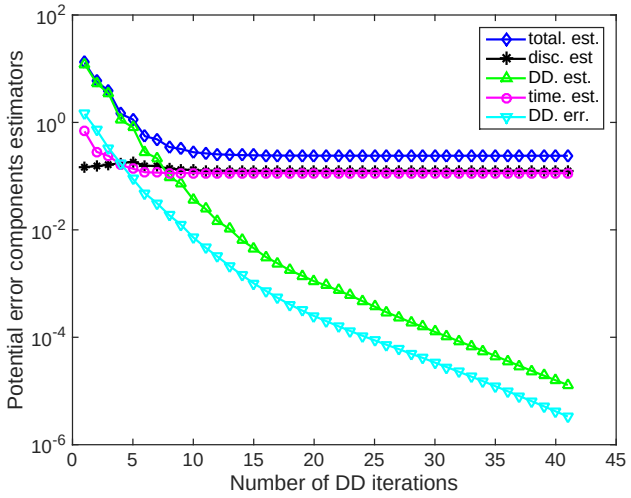

Figure 7: Error component estimates with the GMRES solver

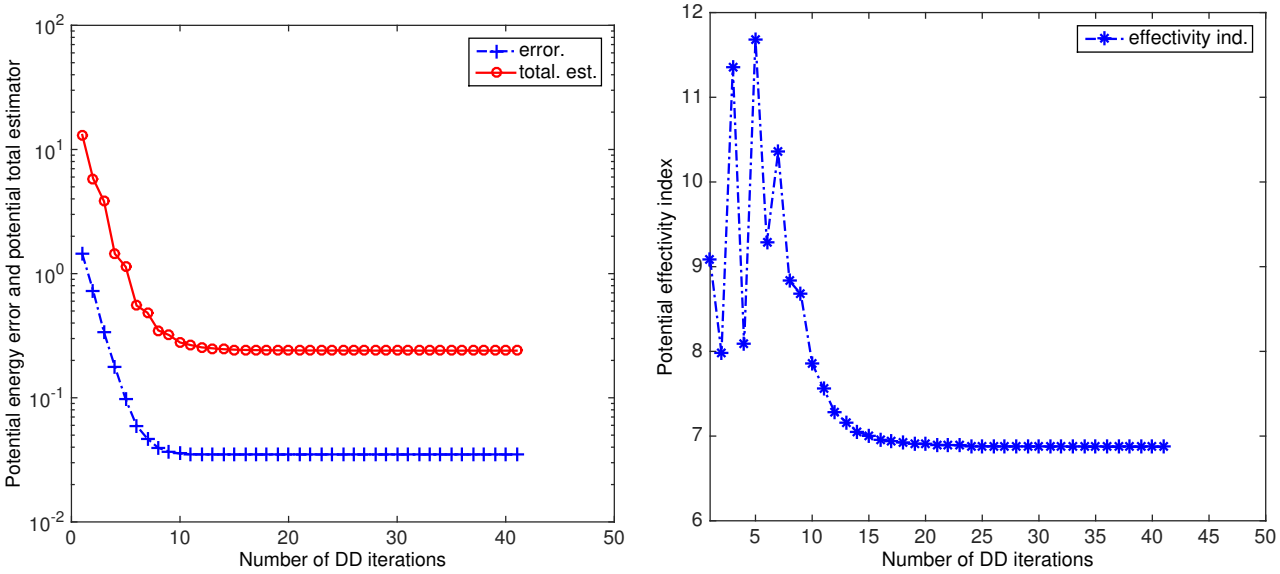

Figure 8: Energy error and total estimator (left), and effectivity index (right), with the GMRES solver

[3] S. Ali Hassan, C. Japhet, M. Kern, and M. Vohralík. A posteriori stopping criteria for optimized Schwarz domain decomposition algorithms in mixed formulations. HAL Preprint 01529532, submitted for publication, 2017.

[4] S. Ali Hassan, C. Japhet, and M. Vohralík. A posteriori stopping criteria for space-time domain decomposition for the heat equation in mixed formulations . HAL Preprint 01586862, submitted for publication, 2017.

[5] T. Arbogast and Z. Chen. On the implementation of mixed methods as nonconforming methods for second-order elliptic problems. *Math. Comp.*, 64(211):943–972, 1995.

[6] M. Arioli. A stopping criterion for the conjugate gradient algorithms in a finite element method framework. *Numer. Math.*, 97(1):1–24, 2004.

[7] M. Arioli and D. Loghin. Stopping criteria for mixed finite element problems. *Electron. Trans. Numer. Anal.*, 29:178–192, 2007/08.

[8] D. N. Arnold and F. Brezzi. Mixed and nonconforming finite element methods: implementation, post-processing and error estimates. *RAIRO Modél. Math. Anal. Numér.*, 19(1):7–32, 1985.

[9] R. Becker, C. Johnson, and R. Rannacher. Adaptive error control for multigrid finite element methods. *Computing*, 55(4):271–288, 1995.

[10] D. Bennequin, M. J. Gander, and L. Halpern. A homographic best approximation problem with application to optimized Schwarz waveform relaxation. *Math. Comp.*, 78(265):185–223, 2009.

[11] E. Blayo, L. Debreu, and F. Lemarié. Toward an optimized global-in-time Schwarz algorithm for diffusion equations with discontinuous and spatially variable coefficients. Part 1: the constant coefficients case. *ETNA, Kent State University Library*, 40:170–186, 2013.

[12] C. Cancès, I. S. Pop, and M. Vohralík. An a posteriori error estimate for vertex-centered finite volume discretizations of immiscible incompressible two-phase flow. *Math. Comp.*, 83(285):153–188, 2014.

[13] L. C. Cowsar, J. Mandel, and M. F. Wheeler. Balancing domain decomposition for mixed finite elements. *Math. Comp.*, 64(211):989–1015, 1995.

[14] F. Cuvelier. Personal communication.

[15] D. A. Di Pietro, E. Flauraud, M. Vohralík, and S. Yousef. A posteriori error estimates, stopping criteria, and adaptivity for multiphase compositional Darcy flows in porous media. *J. Comput. Phys.*, 276:163–187, 2014.

[16] D. A. Di Pietro, M. Vohralík, and S. Yousef. An a posteriori-based, fully adaptive algorithm with adaptive stopping criteria and mesh refinement for thermal multiphase compositional flows in porous media. *Computers & Mathematics with Applications*, 68(12, Part B):2331 – 2347, 2014. Advances in Computational Partial Differential Equations.

[17] V. Dolean, P. Jolivet, and F. Nataf. *An introduction to domain decomposition methods*. Society for Industrial and Applied Mathematics (SIAM), Philadelphia, PA, 2015. Algorithms, theory, and parallel implementation.

[18] V. Dolejší, A. Ern, and M. Vohralík. *hp*-adaptation driven by polynomial-degree-robust a posteriori error estimates for elliptic problems. *SIAM J. Sci. Comput.*, 38(5):A3220–A3246, 2016.

[19] A. Ern, I. Smears, and M. Vohralík. Guaranteed, locally space-time efficient, and polynomial-degree robust a posteriori error estimates for high-order discretizations of parabolic problems. *SIAM J. Numer. Anal.*, 2017. Accepted for publication.

[20] A. Ern and M. Vohralík. A posteriori error estimation based on potential and flux reconstruction for the heat equation. *SIAM J. Numer. Anal.*, 48(1):198–223, 2010.

[21] A. Ern and M. Vohralík. Adaptive inexact Newton methods with a posteriori stopping criteria for nonlinear diffusion PDEs. *SIAM J. Sci. Comput.*, 35(4):A1761–A1791, 2013.

[22] A. Ern and M. Vohralík. Polynomial-degree-robust a posteriori estimates in a unified setting for conforming, nonconforming, discontinuous Galerkin, and mixed discretizations. *SIAM J. Numer. Anal.*, 53(2):1058–1081, 2015.

[23] C. Farhat and F.-X. Roux. A method of finite element tearing and interconnecting and its parallel solution algorithm. *Internat. J. Numer. Methods Engrg.*, 32(6):1205–1227, 1991.

[24] M. J. Gander. Optimized Schwarz methods. *SIAM J. Numer. Anal.*, 44(2):699–731, 2006.

[25] M. J. Gander, L. Halpern, and M. Kern. A Schwarz waveform relaxation method for advection-diffusion-reaction problems with discontinuous coefficients and non-matching grids. In *Domain decomposition methods in science and engineering XVI*, volume 55 of *Lect. Notes Comput. Sci. Eng.*, pages 283–290. Springer, Berlin, 2007.

[26] M. J. Gander, L. Halpern, and F. Nataf. Optimal Schwarz waveform relaxation for the one dimensional wave equation. *SIAM J. Numer. Anal.*, 41(5):1643–1681, 2003.

[27] L. Halpern, C. Japhet, and J. Szeftel. Optimized Schwarz waveform relaxation and discontinuous Galerkin time stepping for heterogeneous problems. *SIAM J. Numer. Anal.*, 50(5):2588–2611, 2012.

[28] T.-T.-P. Hoang, J. Jaffré, C. Japhet, M. Kern, and J. E. Roberts. Space-time domain decomposition methods for diffusion problems in mixed formulations. *SIAM J. Numer. Anal.*, 51(6):3532–3559, 2013.

[29] T.-T.-P. Hoang, C. Japhet, M. Kern, and J. E. Roberts. Space-time domain decomposition for reduced fracture models in mixed formulation. *SIAM J. Numer. Anal.*, 54(1):288–316, 2016.

[30] T. T. P. Hoang, C. Japhet, M. Kern, and J. E. Roberts. Space-time domain decomposition for advection-diffusion problems in mixed formulations. *Math. Comput. Simulation*, 137:366–389, 2017.

[31] C. Japhet and F. Nataf. The best interface conditions for domain decomposition methods: absorbing boundary conditions. In *Absorbing Boundaries and Layers, Domain Decomposition Methods*, pages 348–373. Nova Sci. Publ., Huntington, NY, 2001.

[32] P. Jiránek, Z. Strakoš, and M. Vohralík. A posteriori error estimates including algebraic error and stopping criteria for iterative solvers. *SIAM J. Sci. Comput.*, 32(3):1567–1590, 2010.

[33] K. Y. Kim. A posteriori error analysis for locally conservative mixed methods. *Math. Comp.*, 76(257):43–66, 2007.

[34] P. Ladevèze and J.-P. Pelle. *Mastering calculations in linear and nonlinear mechanics*. Mechanical Engineering Series. Springer-Verlag, New York, 2005. Translated from the 2001 French original by Theofanis Strouboulis.

[35] P.-L. Lions. On the Schwarz alternating method. III: a variant for nonoverlapping subdomains. In R. G. J. P. T. F. Chan and O. Widlund, editors, *Third International Symposium on Domain Decomposition Methods for Partial Differential Equations, held in Houston, Texas, March 20-22, 1989*, pages 202–223. Philadelphia, PA, SIAM, 1990.

[36] J. Mandel. Balancing domain decomposition. *Comm. Numer. Methods Engrg.*, 9(3):233–241, 1993.

[37] V. Martin. An optimized Schwarz waveform relaxation method for the unsteady convection diffusion equation in two dimensions. *Appl. Numer. Math.*, 52(4):401–428, 2005.

[38] D. Meidner, R. Rannacher, and J. Vihharev. Goal-oriented error control of the iterative solution of finite element equations. *J. Numer. Math.*, 17(2):143–172, 2009.

[39] A. T. Patera and E. M. Rønquist. A general output bound result: application to discretization and iteration error estimation and control. *Math. Models Methods Appl. Sci.*, 11(4):685–712, 2001.

[40] G. V. Pencheva, M. Vohralík, M. F. Wheeler, and T. Wildey. Robust a posteriori error control and adaptivity for multiscale, multinumerics, and mortar coupling. *SIAM J. Numer. Anal.*, 51(1):526–554, 2013.

[41] W. Prager and J. L. Synge. Approximations in elasticity based on the concept of function space. *Quart. Appl. Math.*, 5:241–269, 1947.

[42] S. Repin. *A posteriori estimates for partial differential equations*, volume 4 of *Radon Series on Computational and Applied Mathematics*. Walter de Gruyter GmbH & Co. KG, Berlin, 2008.

[43] V. Rey, P. Gosselet, and C. Rey. Strict bounding of quantities of interest in computations based on domain decomposition. *Comput. Methods Appl. Mech. Engrg.*, 287:212–228, 2015.

[44] V. Rey, P. Gosselet, and C. Rey. Strict lower bounds with separation of sources of error in non-overlapping domain decomposition methods. *Internat. J. Numer. Methods Engrg.*, 108(9):1007–1029, 2016.

[45] V. Rey, C. Rey, and P. Gosselet. A strict error bound with separated contributions of the discretization and of the iterative solver in non-overlapping domain decomposition methods. *Comput. Methods Appl. Mech. Engrg.*, 270:293–303, 2014.

[46] V. Thomee. *Galerkin Finite Element Methods for Parabolic Problems*. Springer, 1997.

[47] R. Verfürth. A posteriori error estimates for finite element discretizations of the heat equation. *Calcolo*, 40(3):195–212, 2003.

[48] M. Vohralík. A posteriori error estimates for lowest-order mixed finite element discretizations of convection-diffusion-reaction equations. *SIAM J. Numer. Anal.*, 45(4):1570–1599, 2007.

[49] M. Vohralík. Unified primal formulation-based a priori and a posteriori error analysis of mixed finite element methods. *Math. Comp.*, 79(272):2001–2032, 2010.